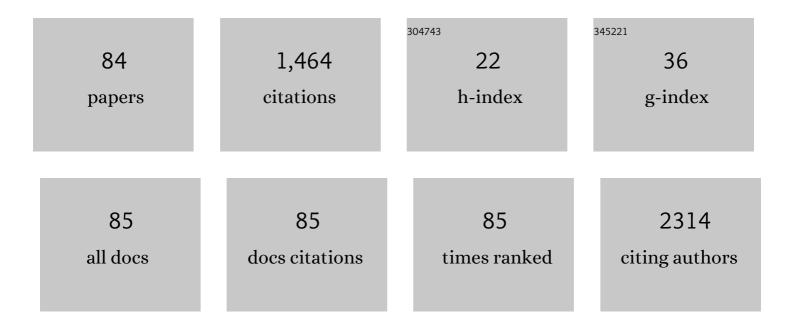
Charudatta Phatak

List of Publications by Year in descending order

Source: https://exaly.com/author-pdf/6669122/publications.pdf Version: 2024-02-01



#	Article	IF	CITATIONS
1	Nanostructure refinement and phase formation of flash annealed FeNi-based soft magnetic alloys. Materials Research Bulletin, 2022, 152, 111839.	5.2	3
2	Geometric control of emergent antiferromagnetic order in coupled artificial spin ices. Cell Reports Physical Science, 2022, 3, 100846.	5.6	1
3	Field-Dependent Magnetic Domain Behavior in van der Waals Fe3GeTe2. Jom, 2022, 74, 2310-2318.	1.9	4
4	Local Multimodal Electroâ€Chemicalâ€Structural Characterization of Solidâ€Electrolyte Grain Boundaries. Advanced Energy Materials, 2021, 11, 2003309.	19.5	7
5	Understanding the Selective Deposition of Li Metal on Nonuniform Electrode Surfaces Using Atomic Force Microscopy. Journal of the Electrochemical Society, 2021, 168, 020534.	2.9	0
6	Understanding Complex Magnetic Spin Textures with Simulation-Assisted Lorentz Transmission Electron Microscopy. Physical Review Applied, 2021, 15, .	3.8	31
7	Understanding curvature effects on the magnetization reversal of patterned permalloy Archimedean spirals. Applied Physics Letters, 2021, 118, .	3.3	8
8	Magnetostrictive loss reduction through stress relief annealing in an FeNi-based metal amorphous nanocomposite. Journal of Materials Research, 2021, 36, 2843-2855.	2.6	9
9	Mesoscale Confinement Effects and Emergent Quantum Interference in Titania Antidot Thin Films. ACS Nano, 2021, 15, 12935-12944.	14.6	1
10	Differential programming enabled functional imaging with Lorentz transmission electron microscopy. Npj Computational Materials, 2021, 7, .	8.7	13
11	Behavior of thermally quenched topological defects in quasicrystal artificial spin ices. Physical Review B, 2021, 104, .	3.2	0
12	Quantifying leakage fields at ionic grain boundaries using off-axis electron holography. Journal of Applied Physics, 2020, 128, .	2.5	2
13	Electron Holography Investigation of Resistive Switching CeO2 / STO Nanocolumns. Microscopy and Microanalysis, 2020, 26, 1950-1951.	0.4	0
14	Variability and origins of grain boundary electric potential detected by electron holography and atom-probe tomography. Nature Materials, 2020, 19, 887-893.	27.5	72
15	Curved Three-Dimensional Cobalt Nanohelices for Use in Domain Wall Device Applications. ACS Applied Nano Materials, 2020, 3, 6009-6016.	5.0	14
16	Exploring the Local Energy Landscape of Aperiodic Artificial Spin Ices via Lorentz TEM. Microscopy and Microanalysis, 2020, 26, 1770-1771.	0.4	0
17	Insights into Lithium Surface: Stable Cycling by Controlled 10 μm Deep Surface Relief, Reinterpreting the Natural Surface Defect on Lithium Metal Anode. ACS Applied Energy Materials, 2019, 2, 5656-5664.	5.1	16
18	Understanding Curvature Effects on Magnetic Domains in 3D Nanostructures. Microscopy and Microanalysis, 2019, 25, 26-27,	0.4	1

#	Article	IF	CITATIONS
19	Effect of the dielectric constant of a liquid electrolyte on lithium metal anodes. Electrochimica Acta, 2019, 300, 299-305.	5.2	27
20	Emergent magnetic ordering and topological frustration in quasicrystal artificial spin ices. Physical Review B, 2019, 99, .	3.2	8
21	Quantifying chiral exchange interaction for Néel-type skyrmions via Lorentz transmission electron microscopy. Physical Review B, 2019, 99, .	3.2	21
22	Effect of nanopatterning on mechanical properties of Lithium anode. Scientific Reports, 2018, 8, 2514.	3.3	33
23	Ferroelectric Domain Studies of Patterned (001) BiFeO3 by Angle-Resolved Piezoresponse Force Microscopy. Scientific Reports, 2018, 8, 203.	3.3	9
24	Reduced electron exposure for energy-dispersive spectroscopy using dynamic sampling. Ultramicroscopy, 2018, 184, 90-97.	1.9	12
25	Topological Defects and Interaction of Electron Waves and Localized Magnetic Charge. Microscopy and Microanalysis, 2018, 24, 940-941.	0.4	1
26	Size effects of micro-pattern on lithium metal surface on the electrochemical performance of lithium metal secondary batteries. Journal of Power Sources, 2018, 408, 136-142.	7.8	20
27	Observation of transient states during magnetization reversal in a quasicrystal artificial spin ice. Physical Review B, 2018, 98, .	3.2	11
28	Direct Evidence of Topological Defects in Electron Waves through Nanoscale Localized Magnetic Charge. Nano Letters, 2018, 18, 6989-6994.	9.1	2
29	SLADS-Net: Supervised Learning Approach for Dynamic Sampling using Deep Neural Networks. IS&T International Symposium on Electronic Imaging, 2018, 30, 131-1-1316.	0.4	5
30	Correlative Magnetic Imaging of Heat-Assisted Magnetic Recording Media in Cross Section Using Lorentz TEM and MFM. IEEE Transactions on Magnetics, 2018, 54, 1-5.	2.1	1
31	In-situ Electron Holography Study of Grain Boundaries in Cerium Oxide. Microscopy and Microanalysis, 2018, 24, 1466-1467.	0.4	0
32	Correlative SPM/TEM Investigation of the Electrochemical Deposition of Lithium Metal. Microscopy and Microanalysis, 2018, 24, 1524-1525.	0.4	0
33	Imaging Magnetic Domains in Functional Nanoscale Heterostructures using Lorentz microscopy. Microscopy and Microanalysis, 2018, 24, 910-911.	0.4	0
34	3D reconstruction of magnetization from dichroic soft X-ray transmission tomography. Journal of Synchrotron Radiation, 2018, 25, 1144-1152.	2.4	17
35	Model-Based Iterative Reconstruction of Magnetization Using Vector Field Electron Tomography. IEEE Transactions on Computational Imaging, 2018, 4, 432-446.	4.4	3
36	A convolutional neural network approach to calibrating the rotation axis for X-ray computed tomography. Journal of Synchrotron Radiation, 2017, 24, 469-475.	2.4	59

#	Article	IF	CITATIONS
37	Under-sampling and Image Reconstruction for Scanning Electron Microscopes. Microscopy and Microanalysis, 2017, 23, 136-137.	0.4	2
38	Magnetic vortex nucleation/annihilation in artificial-ferrimagnet microdisks. Journal of Applied Physics, 2017, 122, 083903.	2.5	5
39	Honeycomb Networks of Metal Oxides from Self-Assembling PS-PMMA Block Copolymers. Microscopy and Microanalysis, 2017, 23, 1654-1655.	0.4	Ο
40	Long-range Stripe Nanodomains in Epitaxial (110) BiFeO3 Thin Films on (100) NdGaO3 Substrate. Scientific Reports, 2017, 7, 4857.	3.3	23
41	3D reconstruction of the magnetic vector potential using model based iterative reconstruction. Ultramicroscopy, 2017, 182, 131-144.	1.9	12
42	Modified Transport-of-Intensity Approach for Mapping In-situ Magnetic Induction. Microscopy and Microanalysis, 2017, 23, 930-931.	0.4	0
43	Tailoring magnetic skyrmions by geometric confinement of magnetic structures. Applied Physics Letters, 2017, 111, 242405.	3.3	8
44	Learning From Scanning Transmission Electron Microscopy to Enhance Transmission X-ray Microscopy: How We Can Merge STEM and TXM Datasets?. Microscopy and Microanalysis, 2016, 22, 240-241.	0.4	1
45	Iterative Reconstruction of the Magnetization and Charge Density using Vector Field Electron Tomography. Microscopy and Microanalysis, 2016, 22, 1686-1687.	0.4	2
46	Domain behavior in functional materials studied using Lorentz microscopy. Microscopy and Microanalysis, 2016, 22, 1680-1681.	0.4	0
47	Creation of artificial skyrmions and antiskyrmions by anisotropy engineering. Scientific Reports, 2016, 6, 31248.	3.3	46
48	Real-space observation of magnetic excitations and avalanche behavior in artificial quasicrystal lattices. Scientific Reports, 2016, 6, 34384.	3.3	24
49	Visualization of Magnetization in CoFe Nanofibers by Lorentz TEM and Electron Holography. Microscopy and Microanalysis, 2016, 22, 1692-1693.	0.4	1
50	Nanoscale Skyrmions in a Nonchiral Metallic Multiferroic: Ni ₂ MnGa. Nano Letters, 2016, 16, 4141-4148.	9.1	79
51	Zig-zag Self-assembly of Magnetic Octahedral Fe3O4 Nanocrystals using in situ Liquid Transmission Electron Microscopy. Microscopy and Microanalysis, 2016, 22, 36-37.	0.4	8
52	Quantitative 3D electromagnetic field determination of 1D nanostructures from single projection. Ultramicroscopy, 2016, 164, 24-30.	1.9	7
53	Recent advances in Lorentz microscopy. Current Opinion in Solid State and Materials Science, 2016, 20, 107-114.	11.5	53
54	Ferromagnetic domain behavior and phase transition in bilayer manganites investigated at the nanoscale. Physical Review B, 2015, 92, .	3.2	5

#	Article	IF	CITATIONS
55	Three dimensional magnetic field reconstruction of artificial Skyrmion heterostructures. Microscopy and Microanalysis, 2015, 21, 1959-1960.	0.4	0
56	Three Dimensional Visualization of Electromagnetic Fields from One Dimensional Nanostructures. Microscopy and Microanalysis, 2015, 21, 1977-1978.	0.4	0
57	Towards Multiresolution Phase Retrieval using Electron Ptychography. Microscopy and Microanalysis, 2015, 21, 2151-2152.	0.4	0
58	Enhancement of Local Piezoresponse in Polymer Ferroelectrics <i>via</i> Nanoscale Control of Microstructure. ACS Nano, 2015, 9, 1809-1819.	14.6	65
59	Iterative reconstruction of magnetic induction using Lorentz transmission electron tomography. Ultramicroscopy, 2015, 150, 54-64.	1.9	16
60	Vortex jump behavior in coupled nanomagnetic heterostructures. Applied Physics Letters, 2014, 105, 212409.	3.3	4
61	Bipolar resistance switching in Pt/CuOx/Pt via local electrochemical reduction. Applied Physics Letters, 2014, 104, .	3.3	19
62	Theoretical study of ferroelectric nanoparticles using phase reconstructed electron microscopy. Physical Review B, 2014, 89, .	3.2	3
63	Dielectric behavior related to TiOx phase change to TiO2 in TiOx/Al2O3 nanolaminate thin films. MRS Communications, 2014, 4, 67-72.	1.8	4
64	Separation of electrostatic and magnetic phase shifts using a modified transport-of-intensity equation. Ultramicroscopy, 2014, 139, 5-12.	1.9	19
65	X-ray Irradiation Induced Reversible Resistance Change in Pt/TiO ₂ /Pt Cells. ACS Nano, 2014, 8, 1584-1589.	14.6	32
66	Visualization of the Magnetic Structure of Sculpted Three-Dimensional Cobalt Nanospirals. Nano Letters, 2014, 14, 759-764.	9.1	73
67	Interface-controlled high dielectric constant Al2O3/TiOx nanolaminates with low loss and low leakage current density for new generation nanodevices. Journal of Applied Physics, 2013, 114, .	2.5	25
68	Tailoring dielectric relaxation in ultra-thin high-dielectric constant nanolaminates for nanoelectronics. Applied Physics Letters, 2013, 102, .	3.3	25
69	Real and effective thermal equilibrium in artificial square spin ices. Physical Review B, 2013, 87, .	3.2	40
70	Magnetic interactions and reversal of artificial square spin ices. New Journal of Physics, 2012, 14, 075028.	2.9	22
71	Direct Observation of Unconventional Topological Spin Structure in Coupled Magnetic Discs. Physical Review Letters, 2012, 108, 067205.	7.8	65
72	On the magnetostatics of chains of magnetic nanoparticles. Journal of Magnetism and Magnetic Materials, 2011, 323, 2912-2922.	2.3	23

#	ARTICLE	IF	CITATIONS
73	In situ Lorentz TEM magnetization studies on a Fe–Pd–Co martensitic alloy. Acta Materialia, 2011, 59, 6646-6657.	7.9	26
74	In situ lorentz TEM magnetization study of a Ni–Mn–Ga ferromagnetic shape memory alloy. Acta Materialia, 2011, 59, 4895-4906.	7.9	35
75	Nanoscale structure of the magnetic induction at monopole defects in artificial spin-ice lattices. Physical Review B, 2011, 83, .	3.2	96
76	Domain Observations in Fe-Pd-Co by Dynamic in-situ Lorentz TEM. Microscopy and Microanalysis, 2010, 16, 1236-1237.	0.4	1
77	Angle Resolved TEM Imaging of Pt Nanoparticles. Catalysis Letters, 2010, 140, 85-89.	2.6	4
78	Three-Dimensional Study of the Vector Potential of Magnetic Structures. Physical Review Letters, 2010, 104, 253901.	7.8	84
79	Determination of magnetic vortex polarity from a single Lorentz Fresnel image. Ultramicroscopy, 2009, 109, 264-267.	1.9	29
80	Determination of the 3-D Magnetic Vector Potential using Lorentz Transmission Electron Microscopy. Microscopy and Microanalysis, 2009, 15, 134-135.	0.4	1
81	Improved Phase Reconstruction for Magnetic Materials in a Low-Aberration Environment. Microscopy and Microanalysis, 2009, 15, 1276-1277.	0.4	1
82	Vector field electron tomography of magnetic materials: Theoretical development. Ultramicroscopy, 2008, 108, 503-513.	1.9	59
83	Reconstruction of 3D Magnetic Induction Using Lorentz TEM. Microscopy and Microanalysis, 2008, 14, 1054-1055.	0.4	1
84	Aberration Corrected Lorentz Microscopy for Perpendicular Magnetic Recording Media. Microscopy and Microanalysis, 2008, 14, 832-833.	0.4	5

6